Plant Methods

Methodology

A novel fluorescent pH probe for expression in plants

Alexander Schulte[1,2], Inken Lorenzen[2], Markus Böttcher[3,4] and Christoph Plieth*[1]

Address: [1]Zentrum für Biochemie und Molekularbiologie, Universität Kiel, Am Botanischen Garten 9, 24118 Kiel, Germany, [2]Biochemisches Institut, Universität Kiel, Rudolf-Höber-Str. 1, 24098 Kiel, Germany, [3]Botanisches Institut, Universität Kiel, Am Botanischen Garten 9, 24118 Kiel, Germany and [4]Institut für Physiologie, Universität zu Lübeck, Ratzeburger Allee 160, 23538 Lübeck, Germany

Email: Alexander Schulte - aschulte@biochem.uni-kiel.de; Inken Lorenzen - ilorenzen@biochem.uni-kiel.de; Markus Böttcher - boettcher@physio.uni-luebeck.de; Christoph Plieth* - cplieth@zbm.uni-kiel.de

* Corresponding author

Abstract

Background: The pH is an important parameter controlling many metabolic and signalling pathways in living cells. Recombinant fluorescent pH indicators (pHluorins) have come into vogue for monitoring cellular pH. They are derived from the most popular *Aequorea victoria* GFP (*Av*-GFP). Here, we present a novel fluorescent pH reporter protein from the orange seapen *Ptilosarcus gurneyi* (*Pt*-GFP) and compare its properties with pHluorins for expression and use in plants.

Results: pHluorins have a higher pH-sensitivity. However, *Pt*-GFP has a broader pH-responsiveness, an excellent dynamic ratio range and a better acid stability. We demonstrate how *Pt*-GFP expressing *Arabidopsis thaliana* report cytosolic pH-clamp and changes of cytosolic pH in the response to anoxia and salt-stress.

Conclusion: *Pt*-GFP appears to be the better choice when used for *in vivo*-recording of cellular pH in plants.

Introduction

Fluorescent proteins have revolutionized the understanding of cellular event cascades, signal transduction, and structure dynamics [1,2]. The green fluorescent protein from *Aequorea victoria* (*Av*-GFP) is the most popular species used by scientists to date. *Av*-GFP and its corresponding cDNA has been altered many times to give fluorescent proteins of higher quantum efficiency, different spectral characteristics, less temperature sensitivity, improved solubility, and higher expression levels in other organisms [e.g. [3,4]]. Enhanced variants of *Av*-GFP are frequently used to decorate cellular structures and proteins in order to observe shape, location and dynamics *in vivo* [e.g. [5-

12]] or to visualize gene expression and/or activity of promoters or enhancers [13].

One of the advantages of GFPs is their ability to be engineered to indicators for cellular signal transduction studies [e.g. [14-16]]. Engineered GFPs have been used in plants to report cellular concentrations of Ca^{2+}, H^+, Cl^-, and NO_3^- [e.g. [17-23]]. No loading of the indicator is necessary with GFP-based probes and they can be precisely targeted to almost any organelle, compartment or tissue in question [e.g. [8,9,11,12,24]]. This potentially makes GFP-derived probes superior to small molecular weight fluorescent dyes used as ion indicators provided they can

replicate the sensitivity and responsiveness of these probes.

In particular two pH-sensitive variants of *Av*-GFP (so-called pHluorins) have been engineered [25]. These two reporters are called 'ratiometric' and 'ecliptic' pHluorin. They both allow ratiometric *in vivo*-pH recording. Ratiometric pHluorin is a double excitation indicator whereas ecliptic pHluorin has to be used in the double emission mode [21]. The amendments necessary for sufficient expression of *Av*-GFPs in plants (i.e. removal of the cryptic intron, changes to *A. thaliana* codon usage and improvement of solubility) have been combined with the properties of pHluorins. The resulting pH indicators have been successfully expressed and used in *Arabidopsis* [21,26,27].

However, more and more fluorescent proteins (FPs) from other marine organisms are being discovered with other interesting properties [28-35]. Some of these newly discovered FPs unveil advantages when compared with *Av*-GFP variants. We have expressed the GFP from the orange seapen (*Ptilosarcus gurneyi*) in bacteria and plants. Here, we compare ratiometric properties of *Pt*-GFP with those of pHluorins and also with conventional fluorescent dyes often used for ratiometric pH measurements *in vivo*.

The spectrum of a fluorescent ratiometric indicator is in a first approach mainly the sum or overlap of two spectra [36]: First, the spectrum of the free indicator (in case of pH indicators the de-protonated form) and second the spectrum of the bound (protonated) indicator molecules. There are further two different effects on the fluorescence of pH indicators which need to be distinguished when the pH is lowered: First a fluorescence quenching at all wavelengths. Second, the spectral disproportionation (i.e. the attenuation of the spectrum from de-protonated indicator for the benefit of the fluorescence spectrum formed by the protonated molecules). Ratiometric fluorescence measurements have been established to cancel down all side-effects based on variations in indicator concentration, illumination intensity, detector sensitivity etc. [37,38]. So, only the second effect, namely spectral disproportionation is essential and relevant for ratiometry and, in theory, the ratio solely correlates with the analyte concentration (here [H+]). A quenching at all wavelengths can be considered an apparent decrease in indicator concentration and is thus irrelevant for ratiometry.

Here all spectra are presented normalized by their area for three reasons: First, this is a way to uncover all spectral effects relevant for ratiometric measurements. Second, it is the optimal way to present the potential capabilities of the indicator (i.e. best pair of wavelengths, dynamic ratiometric change etc.) when intended for ratiometry and/or ratio

imaging. Third, it does not require an *a-priori*-knowledge of the isosbestic point.

By calculating the so-called minimax spectrum (i.e. the spectrum that is obtained when the minimum fluorescence is substracted from the maximum fluorescence at each wavelength within a scanned set of spectra) it is possible to derive two important indicator characteristics: First, the real isosbestic point is the wavelength where the fluorescence is independent from spectral disproportionation. Here, the minimax spectrum, in theory, is zero with discontinuous slope, but, in practice, approaches a minimum close to zero. Second, the sensitivity of the indicator which is defined here as the integral of the minimax spectrum. The sensitivity is a number in the range between zero and two. It is two when there is no spectral overlap of the protonated and the de-protonated form of the indicator (ideal ratiometric indicator). It approaches zero when the indicator is less suitable for ratiometry. Consequently, the normalized spectra give the real isosbestic point while in the raw data spectra (not given here) this point is shifted by the superposed quench effect and is then distinguished here as 'apparent' isosbestic point.

Results & Discussion
Spectral properties of recombinant pH indicators
Ratiometric fluorescent indicators are typically characterized by a set of fluorescence spectra taken under different analyte concentrations (here: different pH values) and otherwise identical conditions. The normalized spectra (coloured curves in Figure 1) allow to calculate the minimax spectrum (grey lines in Figure 1) and to extract a number of characteristic parameters which give clues about signal quality, signal-to-noise ratio, sensitivity, and the best application range of the indicator and about the optimal optical setting when used *in vivo*. The parameters most relevant for practical work are:

1 The isosbestic points λ_{iso} (precisely, the isoexcitation points in case of a double excitation probe or the isoemission points in case of a double emission probe) are the wavelengths where the fluorescence is independent of the indicated analyte (ion) concentration. Here, the real isosbestic point is distinguished from the apparent isosbestic point.

2 Spectral peaks or shoulders left (λ_1) and right (λ_2) of the isosbestic point λ_{iso} which vary in opposite direction when the analyte concentration is changed.

3 The maximum fluorescence wavelength (λ_{max}) is the peak in the emission spectrum in case of a double excitation indicator (such as ratiometric pHluorin and *Pt*-GFP) and the maximum in the excitation spectrum in case of a double emission indicator (such as ecliptic pHluorin).
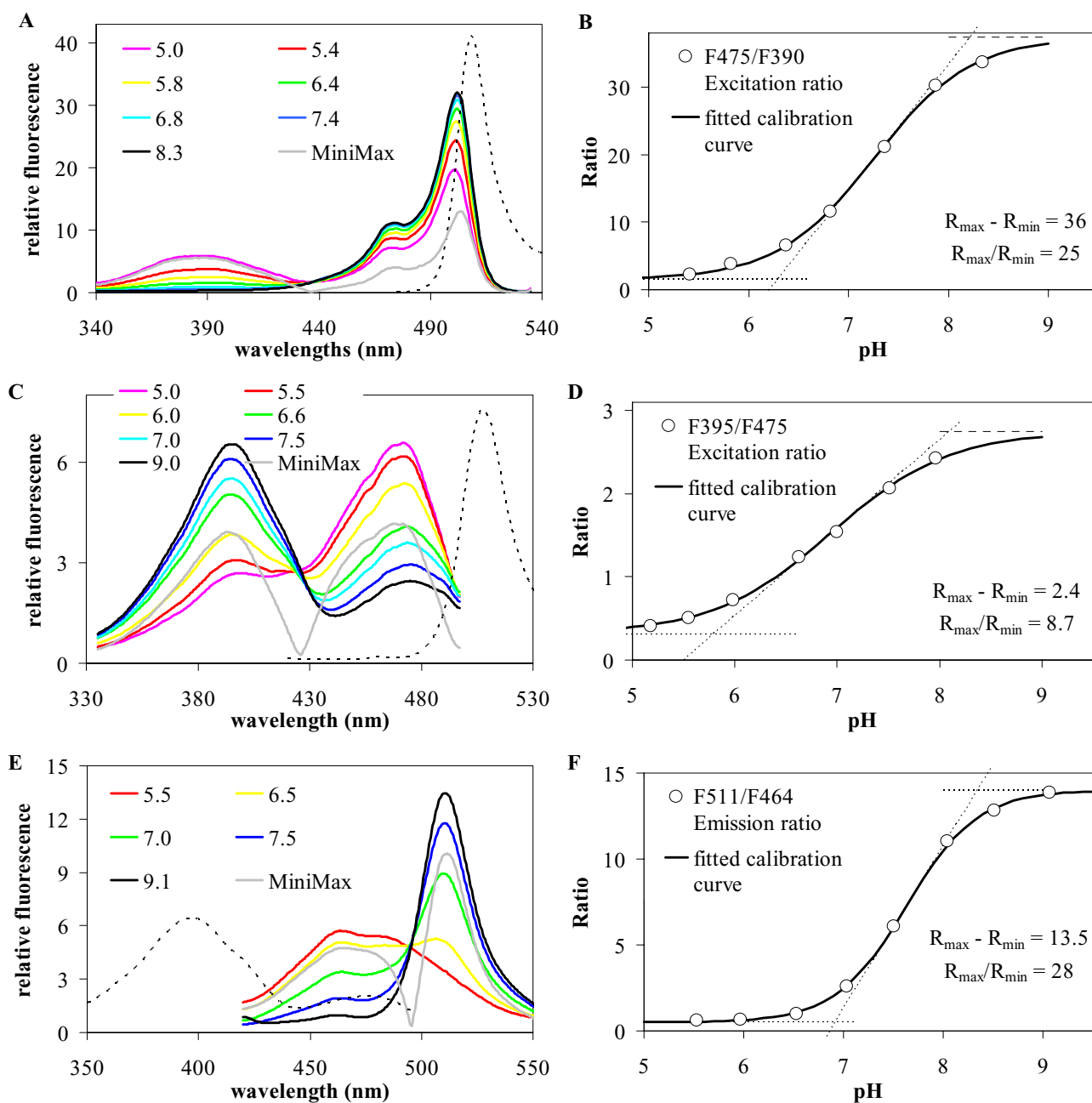
Figure 1
Fluorescence properties of genetically encoded pH-indicators. Spectra taken at different pHs are given for *Pt*-GFP (**A**), ratiometric pHluorin (**C**) and ecliptic pHluorin (**E**). Corresponding ratio curves are on the right hand side (**B, D, F**). **A:** Excitation spectra of *Pt*-GFP at λ_{em} = 540 nm. The dotted line represents the emission spectrum (λ_{ex} = 470 nm) corresponding to pH = 7.4. **B:** Dependency of fluorescence excitation ratios R(475ex/390ex; 540em) of *Pt*GFP on pH. **C:** Excitation spectra of ratiometric pHluorin at λ_{em} = 508 nm. The dotted line represents the emission spectrum (λ_{ex} = 390 nm) corresponding to pH 7.5. **D:** Dependency of fluorescence excitation ratios R(395ex/475ex; 508em) of ratiometric pHluorin on pH. **E:** Emission spectra of ecliptic pHluorin taken at different pH (λ_{ex} = 400 nm). The dotted line represents the excitation spectrum (λ_{em} = 508 nm) corresponding to pH 7.5. **F:** Dependency of fluorescence excitation ratios R(400ex; 511em/464em) of ecliptic pHluorin on pH. All spectra are normalized by their area. The grey curve in each set of spectra (**A, C, E**) represents the corresponding mini-max spectrum (maximum fluorescence difference for each wavelength). Its minimum designates the isosbestic point. Ratio data (**B, D, F**) were fitted with a sigmoidal Boltzmann fit.

4 The Stokes-shift of a fluorescent probe is defined by the difference between the wavelength of its absorption peak (Figure 2) and the wavelength of its emission peak (Figure 1).

5 The maximum and minimum ratios, R_{max} and R_{min} (i.e. the ratios taken in the absence of the analyte or when the indicator is saturated with analyte).

6 The apparent pK (i.e. midpoint of the calibration curve where the ratio reaches half maximum between R_{min} and R_{max}) is dependent on the ratiometric wavelengths chosen (see supplemental data in additional file 1). Ideally, the apparent pK is about the dissociation constant which is defined by the analyte concentration where the indicator is half-saturated.

7 The useful concentration range (x-axis range) in which the indicator is reasonably applied and where the logarithm of the ratio depends approximately linear on the logarithm of analyte concentration. In the case of pH-indicators this range is given by the pH values where the straight line through the midpoint of the logarithmic calibration curve intersects with $\log(R_{max})$ and $\log(R_{min})$ (Figure 3).

8 The sensitivity S of the indicator is defined here (see introduction section) by the area or integral of the mini-max spectrum. The sensitivity is excellent when S > 0.5 (Table 1) and it is negligible when S < 0.1 (Table 4).

The parameters for the three pH-reporter proteins discussed here, namely *Pt*-GFP, ratiometric, and ecliptic pHluorin are given for comparison in Tables 1 and 2. Spectra and calibration curves are depicted in Figure 1. Parameters of some chemical fluorescent dyes often used as ratiometric *in vivo* pH indicators are given for further comparison in an additional file (Table).

When doing ratio imaging, a maximum dynamic fluorescence ratio range (i.e. a maximum fold fluorescence ratio increase R_{max}/R_{min}) is desired in order to gain an optimal signal to noise ratio. However, the experimental conditions – in particular the spectral characteristics of the available filter set and/or dichroic mirror – are often not optimised for the ratiometric probe in use or the Stokes-shift of the indicator is too small for reliably separating fluorescence emission from excitation light. In case of *Pt*-GFP, for instance, the Stokes-shift is just 6 nm (i.e. right excitation peak λ_2 = 502 nm; maximum emission λ_{max} = 508 nm; see Table 1). This is too close to be separated by conventional microscopic filter sets. Hence, wavelengths other than those giving the maximum dynamic ratio range are compulsorily chosen. Thereby, it should be kept in mind that responsiveness and midpoint of the calibration curve (apparent pK) depend on the two wavelengths chosen for ratio measurements. This effect is demonstrated as supplemental data in additional file 1 (Figure S1, Table S2).

For *in vivo* comparison of ratiometric pHluorin and *Pt*-GFP we used the F475 nm/F390 nm pair for excitation
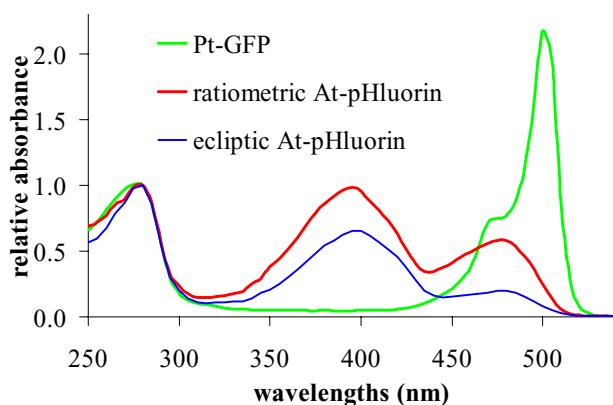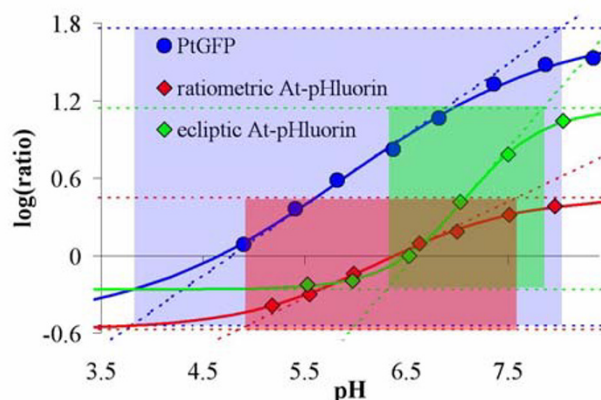

Figure 2
Absorption spectra of pH sensitive GFPs. The spectra were taken in phosphate buffer (pH = 7.4) and normalized by A280. The absorption spectra coincide with the excitation spectra shown in Figures 1.

Figure 3
Comparison of all three recombinant pH-probes on a log-log scale. The areas of best responsiveness are highlighted by coloured rectangles: ecliptic pHluorin in red (emission ratio R_{em} = F511/F465 at λ_{ex} = 400 nm); ratiometric pHluorin in green (excitation ratio R_{ex} = F390/F475 at λ_{em} = 508 nm), and *Pt*-GFP in blue (excitation ratio R_{ex} = F475/F390 at λ_{em} = 540 nm).

Table 1: Spectral characteristics of recombinant pH-probes. The real isosbestic point is derived from normalized spectra whereas the apparent isosbestic point is from the raw data. The Stokes-shifts are defined here by the difference between the wavelength of the major (and the minor) absorption peak and the wavelength of the emission peak. Index 'x' of S designates sensitivity calculated from excitation spectra, and index 'm' values are calculated from emission spectra. 'em', 'ex', and 'abs' designate wavelengths in the emission spectrum, the excitation spectrum, and in the absorption spectrum, respectively.

	GFP-species		
parameter	ratiometric pHluorin	ecliptic pHluorin	*Pt*-GFP
real isosbestic point λ_{iso}	426 nm (ex)	495 nm (em)	437 nm (ex)
apparent isosbestic point	428 nm (ex)	489 nm (em)	430 nm (ex)
left peak WL ($\lambda_1 < \lambda_{iso}$)	395 nm (ex, abs)	464 nm (em)	390 nm (ex)
right peak WL($\lambda_2 > \lambda_{iso}$)	475 nm (ex)	511 nm (em)	502 nm (ex)
Stokes-shift ($\lambda_{em} - \lambda_{abs}$)	113 nm (33 nm)	114 nm (35 nm)	6 nm
maximum WL (λ_{max})	508 nm (em)	397 nm (ex, abs)	508 nm (em)
R_{max} ($F(\lambda_1)/F(\lambda_2)$)	2.75	14	107
R_{min} ($F(\lambda_1)/F(\lambda_2)$)	0.3	0.5	4.2
$R_{max} - R_{min}$	2.44	13.5	103
R_{max}/R_{min}	8.7	27	26
apparent pK (λ_1; λ_2)	6.9	7.6	7.3
Responsiveness ($\Delta\log(R)\cdot\Delta pH$)	2.9	2.0	**9.8**
pH sensitivity (S_x)	**0.77**	0.41	**0.69**
pH sensitivity (S_m)	0.34	**1.05**	0.09

with an emission range between 510 nm ≤ λ_{em} ≤ 560 nm. In Table 2 the optical properties for this particular pair are listed for comparison.

Both, ratiometric and ecliptic pHluorins do not differ significantly in their spectra when other proteins are fused to the N- and/or the C-terminus [21]. This is also true for *Pt*-GFP (unpublished observations). This property is important since fusions with transit or signal peptides are often used to specifically target the indicator to subcellular locations.

For direct comparison of all three pH-probes the ratios where plotted on a log-log-scale (Figure 3). This allows to determine the area of best indicator responsiveness (dynamic ratio range *vs.* dynamic pH range). The diagram (Figure 3) clearly shows that *Pt*-GFP has the best responsiveness ($\Delta\log(R) \cdot pH = 9.8$) and the broadest pH-application range. The responsiveness is lower with ratiometric

Table 2: Comparison of ratiometric pHluorin an *Pt*-GFP when excitation ratios R(F475; F390) are taken. The optimal pH-range is calculated here from a double log-plot as shown in Figure 3

	GFP-species	
parameter	ratiometric pHluorin	*Pt*-GFP
R_{max}	2.65	37.4
R_{min}	0.3	1.5
R_{max}/R_{min}	8.8	25
$R_{max} - R_{min}$	2.35	36
apparent pK (390 nm; 475 nm)	6.9	7.3
optimal pH-range	4.8 < pH < 7.6	3.8 < pH < 8.2

pHluorin (2.9) and ecliptic pHluorin (2.0). *Pt*-GFP responsiveness also exceeds that of conventional pH-indicators (Table S1 in 1). However, *Aequorea* GFPs have a better sensitivity than *Pt*-GFP (Table 1) but the sensitivities of all three recombinant indicators are of similar magnitude (0.65 < S < 1) when compared with conventional dyes (Table S1).

pH-stability of GFPs

The fluorescence quench at all wavelengths by low pH has already been mentioned above. This is due to reversible protonation of *Av*-GFPs in the range 7 > pH > 5 and by irreversible conformational changes leading to protein instability in the range pH < 5 [39,40]. The latter effect is undesirable when GFPs are used as pH-probes in plants. The apoplast of plant cells is usually acidic (pH < 6.5) [21,41,42], and also some vacuoles have low pH. Thus, cytoplasmic pH changes can be drastic in plants (see e.g. *in vivo* experiments below). Therefore it is good to have a pH indicator with high acid stability and ratiometric responsiveness in the lower pH range.

To quantify indicator stability at low pH we recorded GFP fluorescence and its reversibility during low pH-treatment (Figure 4). GFPs from *Aequorea victoria* (*Av*-GFPs) do not recover from a treatment with pH lower than 4 (Figure 4B) whereas *Ptilosarcus* GFP is more stable at low pH and does recover to approx. 40% even after 30 min at pH = 2.5 (Figure 4A). This acid stability of *Pt*-GFP is a special advantageous feature that will allow to overcome difficulties that have been experienced when *Av*-GFP was used for labelling plant vacuoles [8,12]. Together with the broader pH application range *Pt*-GFP can also be used to monitor

Table 4: Comparison of camera exposure times needed for ratiometric pHluorin and *Pt*-GFP when excitation ratios R(F475; F390) are taken in plants under otherwise identical settings.

parameter	GFP-species	
	ratiometric pHluorin	*Pt*-GFP
390 nm	180	300
475 nm	150	100

pH changes in vacuoles and other acidic compartments or in the cytoplasm under conditions when the cellular environment is switched towards the acidic.

Mass properties of recombinant pH indicators

The predicted protein masses of *Pt*-GFP and pHluorins are approximately 27 kDa. We confirmed this by denaturating SDS PAGE (data not shown). However, when native proteins were run on FPLC different masses were detected. *Pt*-GFP exhibited a mass of approx. 105 kDa, whereas pHluorins were detected at around 55 kDa. This indicates the formation of dimers in case of pHluorins and of tetramers in case of *Pt*-GFP.

### Cross-sensitivities of recombinant pH indicators

Cross-sensitivities are often major drawbacks when fluorescent proteins are engineered to indicators for cellular signal transduction studies [19,43]. Therefore fluorescence spectra of all three pH-probes were taken *in vitro* with purified protein to check for possible chloride and redox cross-sensitivities. The chloride sensitivities found (Table 3) in the range of 0 < [Cl-] < 1 M (at pH = 7.5 in 50 mM Hepes) are negligible (i.e. S << 0.1) and there are also no noteworthy spectral differences between reduced and oxidize probes (i.e. 20 mM DTT in degassed PBS *vs.* 50 mM H_2O_2 in PBS).

In vivo properties of recombinant pH indicators

When cDNA encoding *Pt*-GFP is transferred into the genome of *Arabidopsis* under the control of the CaMV 35S promoter, the fluorescent protein is readily expressed in all cells of the plant and distributes well in the cytoplasm (Figure 5). From *Av*-GFP it has been experienced that this is not a matter of course. First, the *Av*-GFP gene was not entirely accepted by *Arabidopsis* and was expressed only after a cryptic intron was removed from the cDNA [3]. Second, the quantum efficiency was poor in the beginning and mutations were introduced to increase the brightness. Third, the distribution in the cytoplasm was found to be inhomogeneous and further amendments were necessary to increase the cytoplasmic solubility of the protein [4]. Both, the high quantum efficiency of *Pt*-GFP [35] (US Patent No. 6,232,107) and its good expression in plants (Figure 5) do not make any alterations of aminoacid sequence or codon usage necessary.

However, quantum efficiency or brightness of GFPs cannot be directly compared *in vivo* since a lower quantum
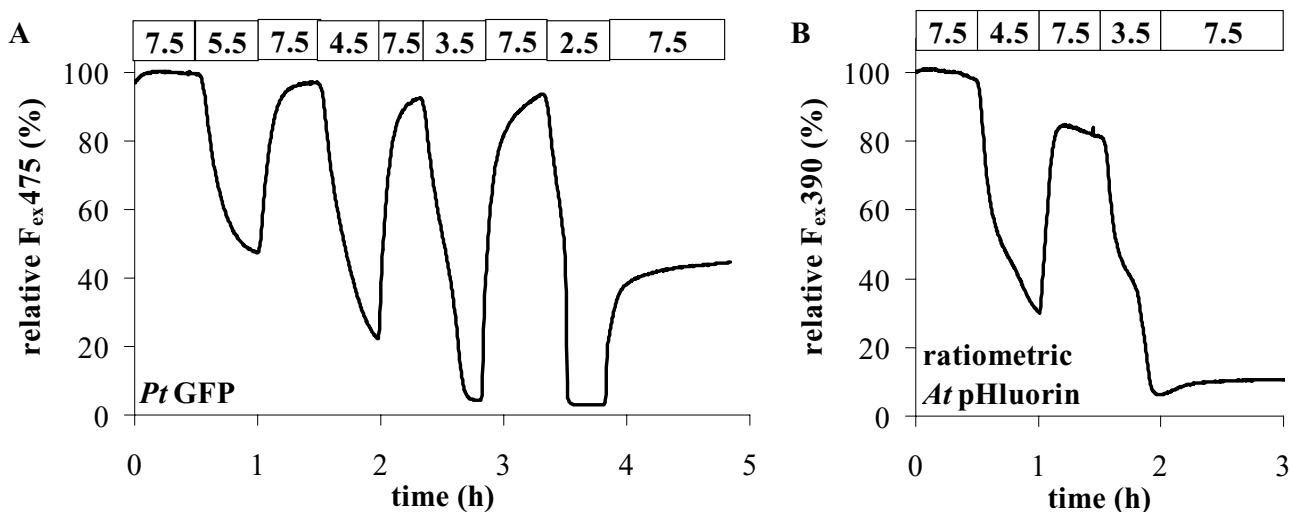
Figure 4
pH-stability of *Pt*-GFP (**A**) and ratiometric pHluorin (**B**). Agarose beads decorated with GFP and sandwiched between sheets of cellophane were dialysed against buffers of different pH as indicated by the top bars of the graphs and fluorescence (F_{em} = 535 ± 25 nm) was recorded with a fluorescence microscope. (Buffer composition: 50 mM Hepes, 50 mM Mes, 200 mM NaCl adjusted with NaOH or HCl to the desired pH).

Table 3: Cross-sensitivities of recombinant pH-probes. Index 'x' designates sensitivity calculated from excitation spectra, and 'm' calculated from emission spectra

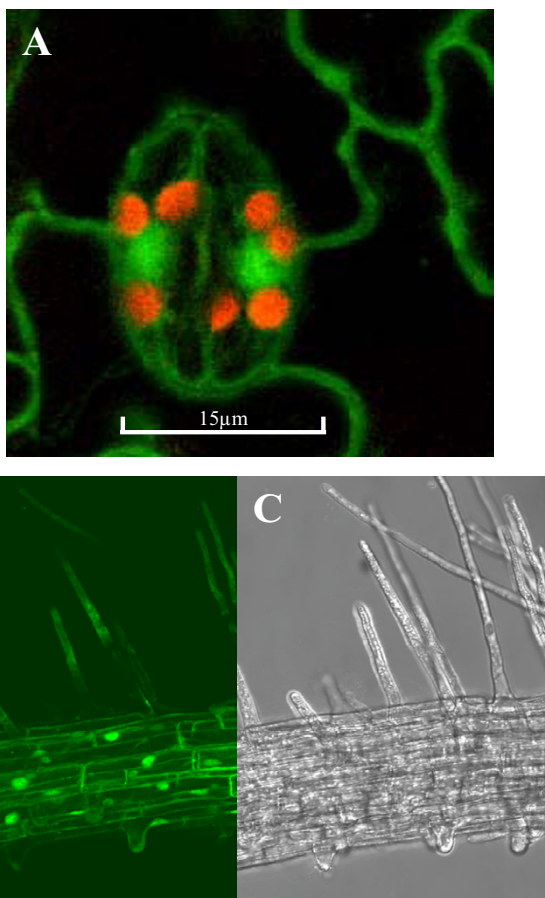| parameter	ratiometric pHluorin	GFP-species ecliptic pHluorin	*Pt*-GFP
S_x (Chloride)	0.03	0.04	0.04
S_m (Chloride)	0.02	0.02	0.02
S_x (red/ox)	0.04	0.05	0.03
S_m (red/ox)	0.01	0.01	0.02

Figure 5
Arabidopsis line expressing *Pt*-GFP. **A:** Confocal image of *Arabidopsis* guard cells expressing *Pt*-GFP in the cytoplasm. The red fluorescence is chlorophyll autofluorescence from chloroplasts. **B:** Confocal optical sections and **C:** corresponding bright-field image of a root segment. Excitation with Argon laser line 476 nm; emission at 500–540 nm (green channel) and 600–660 nm (red channel); Leica TCS SP confocal laser scanning system; HC PL APD objective (40× oil).

efficiency could be compensated by a higher expression level. But, the excitation energy or dose is crucial for practical work because it may lead to photodamage or -bleaching when too high. Therefore, we compared exposure times necessary to reach a reasonable signal at the two wavelengths used for *in vivo* ratiometry (Table 4). CCD camera-based *in vivo* ratio imaging systems allow wavelength-independent adjustments of exposure times.

In Figure 2 absorption is normalized by the protein concentration (i.e. by A280). This allows direct comparison of absorption in the visible and demonstrates that *Pt*-GFP has a higher peak absorption here than pHluorins. This promises the need of lower excitation energy. But its very low absorption at 390 nm requires the F390 nm signal having threefold the exposure time of the F475 nm signal to be in the optimal range (Table 4). Fluorescein derivatives like BCECF and FITC have similar asymmetric spectra like *Pt*-GFP and also require appropriate adjustments. For AtpHluorins in contrast such asymmetric adjustment of exposure times is not needed because of the greater symmetry in their spectra. Hence, the higher quantum efficiency of *Pt*-GFP does not necessarily carry forward in a lower excitation energy needed for balanced signals. A way to circumvent this may be to choose instead of 390 nm a wavelength at or closer to the isosbestic point.

'In situ'-calibration
For converting fluorescence ratio data taken from living cells into pH_{cyt} values, an '*in-situ*' calibration procedure was performed using the same optical set-up as for *in vivo* measurements. Therefore, agar beads were decorated with fluorescent protein, sandwiched between sheets of cellophane and dialysed on the microscope against buffers of different adjusted pH (Figures 6A, B). Ratios were plotted over pH and a sigmoidal curve (Boltzmann function) fitted to the data. The low excitation peak of *Pt*-GFP at 390 nm (Figure 1) could be argued to lead to increased variance in the ratio in particular at physiological pH values when F390 is used as denominator. Such spectral imbalance between the two excitation wavelengths used for ratioing is also found with conventional fluorescein derivatives used for pH measurements like BCECF or FITC. However, the errorbars in Figures 6C and 6D show that the scatter of *Pt*-GFP ratios is negligibly increased when compared with ratiometric pHluorin.

Microenvironmental parameters such as viscosity, hydrophobicity, protein mobility, and binding interactions [44] as well as spectral imbalance can be attributed to shifts in the response of an indicator when going from *in vitro* (spectrometer) to *in situ* or to *in vivo* (microscope) recording. Noticeable here is a shift of the apparent pK when comparing Figures 1B and 6C. However, this is not disas-
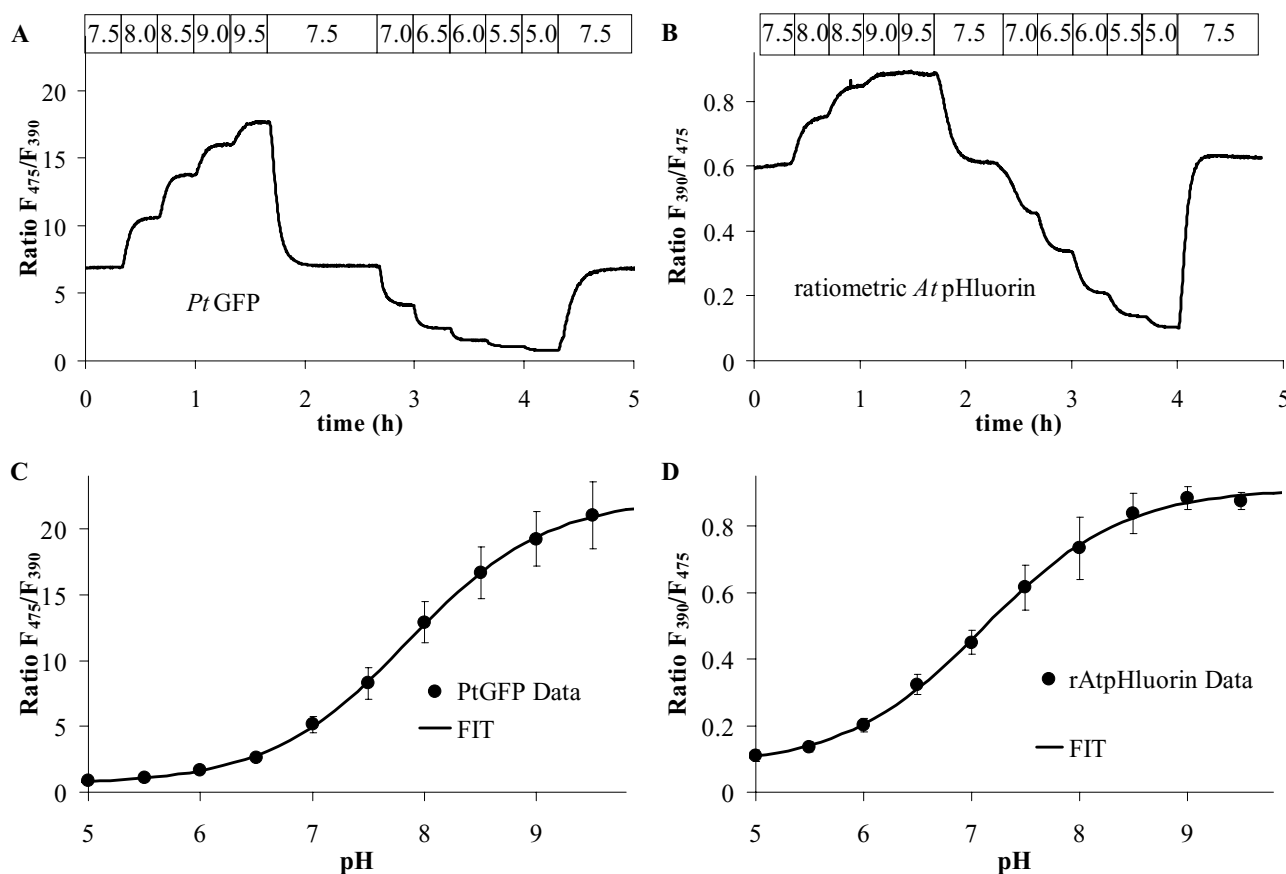
Figure 6
'In situ' calibration procedure. **A, B:** Fluorescence ratio time series of agar beads decorated with *Pt*-GFP (**A**) or ratiometric pHluorin (**B**) during dialysis against buffers of different pH as indicated by the top bar. **C, D:** Resulting calibration curves. Error bars indicate standard deviation. Data in **C** are averages of 9 from 7 individual experiments and data in **D** are averages of 14 from 4 individual experiments.

trous as long as recordings of calibration data and *in vivo* data are identical.

pH-clamp
The cytoplasmic pH in plants is well buffered [45] and strictly regulated [46]. However, it is possible to adjust cytoplasmic pH values different from the cell's set-point by using weak acids [44,45] or weak bases. Here we performed pH-clamp experiments with *Arabidopsis* expressing *Pt*-GFP and ratiometric pHluorin and recorded the cytoplasmic pH (pH_{cyt}) under identical conditions (Figure 7).

Anoxia – an abiotic stimulus that heavily affects cytoplasmic pH
Anoxia is a typical abiotic stress factor that appears for instance in clayey or waterlogged soils. Anoxia is known to produce massive acidification of the cytoplasm. Here we demonstrate how *Arabidopsis* expressing *Pt*-GFP report this effect (Figure 8). Cytoplasmic pH shifts in response to

low oxygen have been reported many times and quantified by different methods [46,47]. Felle [48] used pH-specific microelectrodes and recorded in *Medicago sativa* under anoxia a fall of pH_{cyt} down to 6.8. This is approximately half a pH unit below the normal cytoplasmic level. A shift of similar magnitude was reported from maize roots [49] and from sycamore cells [50] by ^{31}P-NMR. The results presented here (Figure 8) match well with the experiments from Felle [48], Ratcliffe [49], and Gout et al. [50].

Salt stress – an abiotic stimulus that hardly affects cytoplasmic pH
Salt stress is a major stress factor leading to massive cuts in crop yield worldwide ([51]; http://www.plantstress.com). One way to combat this problem is to produce crop plants with improved salt tolerance [52-54]. A pre-requisite for this is to understand ion-transport and the mechanisms underlying salt tolerance on cellular and subcellular level.
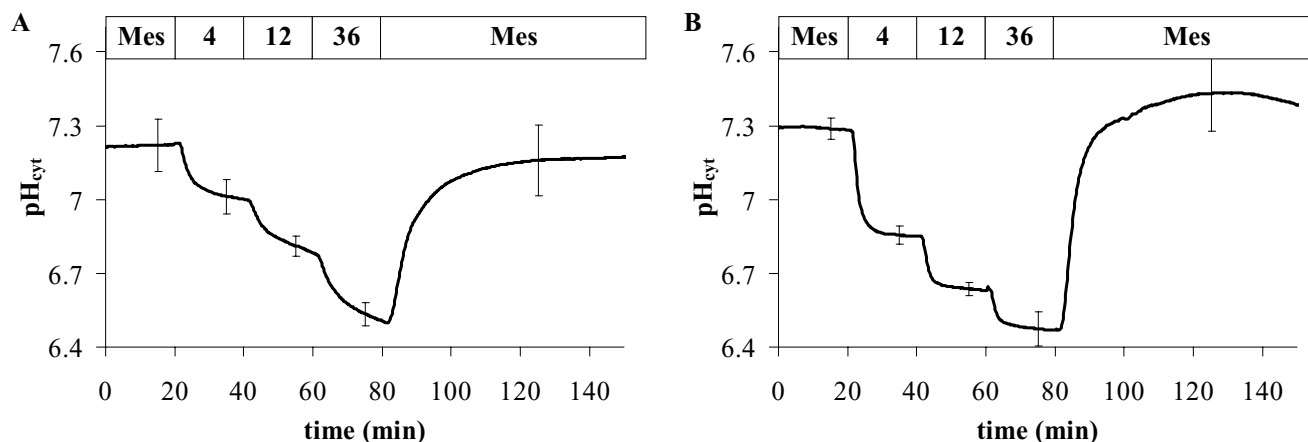
A

B

Figure 7
pH-clamp in *Arabidopsis* root cells (hairy zone near the hypocotyl) expressing *Pt*-GFP (**A**) and ratiometric pHluorin (**B**). Perifusionbuffers were MES-buffer (i.e. KCl, CaCl$_2$, MgCl$_2$ 0.1 mM each, 5 mM MES/NaOH pH 5.4) and supplemented with Na-Butyrate of mM-concentrations as indicated by the top bar of the graphs. Curves are averages of 5 from 3 individual experiments. Error bars indicate standard deviation.

We started to study changes in cellular ion relations under salt stress [21,23]. Here we use *Pt*-GFP expressing *Arabidopsis* to demonstrate how the cytoplasmic pH is affected by increasing concentrations of NaCl (Figure 9). The result coincides well with a similar experiment performed with ratiometric pHluorin [21]. *Arabidopsis* seems to strictly control pH$_{cyt}$ when confronted with salt stress.
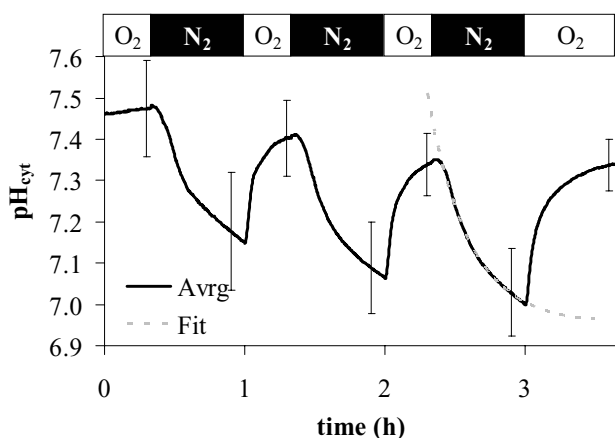

Figure 8
Anoxia-induced pH-deprivation in roots cells (elongation zone near the root tip) of *Arabidopsis* expressing *Pt*-GFP. Given is the average of 7 from 5 individual experiments. Error bars indicate standard deviations. The dotted line gives a first order exponential fit to extrapolate the new predicted steady state pH value (6.95) under anoxia.

Here (Figure 9) NaCl concentrations above 100 mM leads to slight acidification of approx 0.04 pH units. However, a more pronounced acidification of about 0.2 pH units is observed when saltstress is released. This latter effect can be attributed to H$^+$ coupled Na$^+$ export via Na$^+$/H$^+$ antiporter [55]. Other studies on different plant species and conducted with different methods show inconsistent results [55-60]. However, all clearly confirm that salt stress (Figure 9) if at all only slightly (i.e. ΔpH$_{cyt}$ < 0.3) affects pH$_{cyt}$ when compared to anaerobiosis (Figure 8).

Summary
Advantages have been found when comparing Pt-GFP with pHluorins:

1 *Pt*-GFP is readily expressed by *Arabidopsis* without any cDNA modifications (Figure 5). Although the cDNA is derived from a distinct and totally unrelated organism, the codon-usage is accepted by *Arabidopsis* and the plant constitutively expresses the protein with high yield under the control of a single 35S-promotor. The use of *Av*-GFP in higher plants, in contrast, was initially limited. Alterations of the codon usage and the removal of a cryptic intron were found necessary to express *Av*-GFP in *Arabidopsis* [3].

2 *Pt*-GFP is readily soluble and distributes well when expressed in the cytoplasm of plants (Figure 5) whereas for *Av*-GFPs modifications where found beneficial to increase protein solubility in the plant cytoplasm [4].
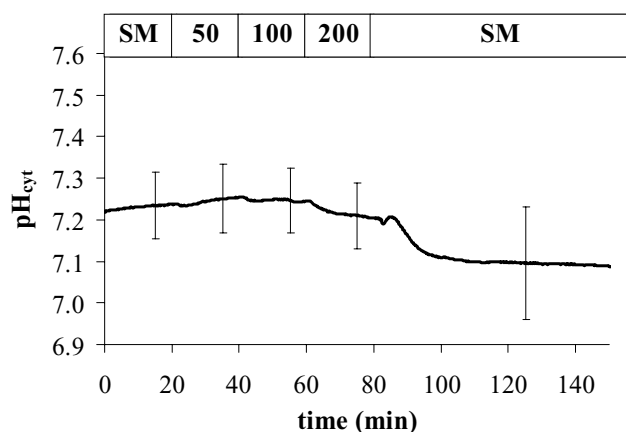
Figure 9
Salt stress-induced pH-changes in roots cells (hairy zone near the hypocotyl) of *Arabidopsis* expressing *Pt*-GFP. Roots were perifused with unbuffered standard medium (SM = KCl, CaCl$_2$, MgCl$_2$ - 0.1 mM each) and millimolar NaCl concentrations as indicated by the top bar of the graph. Given is the average of 5 from 4 individual experiments. Error bars indicate standard deviations.

4 The fluorescence excitation ratio of *Pt*-GFP has a maximum dynamic range (R_{max} - R_{min}) 15 times and a maximum ratio increase (R_{max}/R_{min}) three times higher than that of ratiometric pHluorin when using excitations at 390 nm and 475 nm (Table 2). It further has a broader area of responsiveness (Figure 3) and thereby also exceeds conventional fluorescein derivatives used for ratiometric *in vivo* pH-measurements (supplemental data in 1 Table S1).

5 *Pt*-GFP is much more robust at low pH (Figure 4). This makes it also suitable for monitoring pH in acidic subcellular compartments or under conditions when the cellular pH is shifted towards the acidic.

Taken together, *Pt*-GFP is an excellent pH indicator for excitation fluorescence ratio imaging and in some respects superior to pHluorins when used in plants.

Materials and methods
Standard PCR and cloning techniques [61,62] were employed to engineer all constructs described below. cDNAs coding for pHluorins have been cloned and expressed as described [21].

Bacterial expression, purification, and in vitro-analyses of GFPs
DNA coding for *Pt*-GFP (Acc.No. AY015995) has been subcloned from a pUC18 vector (Nanolight Technologies,

Pinetop, AZ, USA) into the bacterial expression vector pRSETb (Invitrogen GmbH; Karlsruhe, FRG). Protein production was induced with 1 mM IPTG when OD600 = 0.6 and expressed at 20°C/300 rpm over night (i.e. 15 h). For protein isolation bacteria were cracked by sonication (HD2200&MS73, Bandelin, Berlin, Germany) in 200 mM phosphate buffer (pH 7.5). Bacterial lysate was precleared at 4,000 × g for 2 h at 4°C. Remaining debris was removed from the supernatant by filtering through a 0.45 μm nylon filter. The 6xHis-tagged fluorescent protein was purified and concentrated through a Ni^{2+}/NTA-agarose column (Qiagen, Hilden, Germany). Gel filtration through a NAP-25 column (Pharmacia Biotech, Freiburg, Germany) was performed to remove imidazol from the eluted protein. The purified indicator proteins were assessed spectroscopically. Fluorescence spectra (Figure 1) of the proteins were taken with a fluorescence spectrometer (F-2500, Hitachi) in 150 mM KCl and 50 mM appropriate organic buffers (Mes, Pipes, Hepes, Taps) adjusted to the desired pH with NaOH. Absorption spectra (Figure 2) were taken in phosphate buffer (pH = 7.5) with an absorption spectrometer (2100, Hitachi).

Size exclusion chromatography (FPLC)
For FPLC protein was bound to a 0.5 ml column of Toyopearl resin (AF-Chelate-650 M; Tosoh Bioscience) washed with Tris/HCl-buffer (50 mM Tris/HCl pH = 8) and treated with Enterokinase (EKMax, Invitrogen) for 24 h at RT. Protein with His-Tag cleaved was washed from the column with 2 ml 1 × PBS and used for fast protein liquid chromatography (FPLC). Briefly, proteins were subjected to FPLC at 4°C with an HiLoad-16/60 Superdex200 column (Amersham Biosciences), equilibrated with 1 × PBS (Medicago AB; Uppsala, Sweden), pre-fitted with a column guard, and driven by a HPLC pump (Äkta-Explorer; Amersham Biosciences) at a flow rate of 1 ml/min. The column was calibrated using a mixture of four proteins of known molecular mass, i.e. catalase (232 kDa), aldolase (158 kDa), chymotrypsinogen A (25 kDa), and ribonuclease A (13.7 kDa).

Expression in plants
pHluorins for expression in plants were constructed as described in Gao et al. [21]. *Pt*-GFP cDNA (Nanolight Technologies, Pinetop, AZ, USA) was expressed in ecotype Columbia-0 of *Arabidopsis thaliana* under the control of the CaMV 35S promoter using the pART7/pART27 cloning/expression system [63]. Full functionality of *Pt*-GFP in pART7 was assessed by biolistic bombardment and transient expression of young *Arabidopsis* plants (ecotype Col-0) before subcloning the cDNA cassette from pART7 into the binary vector pART27. For agrobacterium-mediated transformation of *Arabidopsis thaliana* (Col-0) the floral dip method [64] was applied.

Confocal laser scanning microscopy (CLSM)

Transient and stable expressions of GFPs (Figures 6) were assessed by CLSM as described [21] using a Leica TCS SP confocal laser scanning system. For *Pt*-GFP excitation the 476 nm beamline of the Argon laser was chosen; emission at 500–540 nm (green channel) for GFP fluorescence and 600–660 nm (red channel) for chlorophyll autofluorescence; HC PL APD objective (40× oil).

In situ-calibration of pH probes

For assessment of acid stability (Figure 4) and for in situ-calibration of the pH-indicators (Figure 6) protein was bound to Ni^{2+}-agarose beads (Qiagen, Hilden, FRG). Fluorescent beads were sandwiched between two layers of cellulose (Cellophane) and dialysed on the microscope against the buffer solutions indicated in figures.

In vivo pH-recording

For *in vivo* recording of fluorescence ratios (Figures 7, 8, 9) transgenic *Arabidopsis* were grown in 9 cm Petri dishes on vertical agar as described [65] and used when 6 to 14 days old. Cytoplasmic pH was measured in the hairy root segments near the hypocotyl. Experimental conditions, perifusion technique, and fixation of plant material were described previously [44]. Roots were placed in a volume of 1.6 ml and perifusion flow was adjusted to 2.4 ml/min. The perifused buffer contained KCl, $MgCl_2$, and $CaCl_2$, 0.1 mM each and 5 mM MES/NaOH adjusted to pH = 5.4. For pH-clamp this buffer was supplemented with different concentrations of sodium butyrate as indicated by the top bar of Figure 7.

Fluorescence ratio imaging

Fluorescence imaging was performed essentially as described [21,23]. Briefly, fluorescence images at excitation wavelengths of 475 nm and 390 nm were taken every 12 s with a ratio imaging system from TILL-Photonics http://www.TILL-photonics.de fitted to an inverted microscope (Diaphot, Nikon) using light from a monochromator (Polychrome IV, TILL). For the emission path a filter block with beamsplitter 500 dcxr and emission filter HQ535/50 (AHF-Analysentechnik, Tübingen, Germany) was used. TILL software (TILLVision 3.3) was used for processing raw data. The fluorescence ratio F475/F390 was taken with *Pt*-GFP and the ratio (F390/F475) was taken with ratiometric pHluorin as a measure for pH.

Data analysis

Each spectrum is normalized by its integral (i.e. the sum of fluorescence values over all wavelengths λ). The minimax spectrum $F_{minimax}(\lambda)$ of a set of spectra is determined by substracting the minimal fluorescence from the maximal fluorescence at each wavelength within the obtained set of spectra (i.e. within the scanned analyte concentration range). The isosbestic point (λ_{iso}) is determined by looking for the minimum in the minimax spectrum. Ideally, the minimax spectrum is zero at the isosbestic point (i.e. $F_{minimax}(\lambda_{iso})$ = 0). The sensitivity S is defined here by the integral of the minimax spectrum. The sensitivity S of each reporter protein is calculated for the set of its excitation spectra (S_x) as well as for its corresponding set of emission spectra (S_m). The Boltzmann fit has been chosen here for fitting sigmoidal curves to calibration data since the Boltzmann equation can directly be derived from the Grynkiewicz equation [66] describing the relation of analyte concentration on fluorescence and fluorescence ratios. The fit parameter of the Boltzmann include R_{min}, R_{max}, and the apparent pK of the calibrated indicator. Fitting has been performed using Origin 7.0 (OriginLab Corp., Northhampton, MA, USA).

Availability of materials

Seeds from *Pt*-GFP expressing *Arabidopsis* are freely available from the European Arabidopsis Stock Centre (Nottingham, UK; http://arabidopsis.info/). All other novel material described in this studies can be obtained for non-commercial purposes from the corresponding author on request.

Abbreviations

Av = Aequorea victoria, *At = Arabidopsis thaliana*, CLSM = confocal laser scanning microscopy, DTT = di-Thiotreitol; FPLC = fast protein liquid chromatography, GFP = green fluorescent protein, Hepes = N-2-hydroxy-ethyl-piperazine-N'-2-ethane-sulfonic acid, Mes = 2-[N-morpholino]-ethane-sulfonic acid, PBS = phosphate buffered saline; *Pt = Ptilosarcus gurneyi*

Competing interests

The author(s) declare that they have no competing interests.

Additional material

> ### Additional file 1
>
> Click here for file
> [http://www.biomedcentral.com/content/supplementary/1746-4811-2-7-s1.pdf]

References

1. Pozzan T: **Calcium turns turquoise into gold.** *Nature* 1997, **388**:834-835.
2. Zhang J, Campbell RE, Ting AY, Tsien RY: **Creating new fluorescent probes for cell biology.** *Nature Reviews Molecular Cell Biology* 2002, **3**:906-918.
3. Haseloff J, Siemering KR, Prasher DC, Hodge S: **Removal of a cryptic intron and subcellular localization of green fluorescent protein are required to mark transgenic *Arabidopsis* plants brightly.** *Proceedings of the National Academy of Science USA* 1997, **94**:2122-2127.
4. Davis SJ, Vierstra RD: **Soluble, high fluorescent variants of green fluorescent protein (GFP) for use in higher plants.** *Plant Molecular Biology* 1998, **36**:521-528.
5. Runions J, Brach T, Kühner S, Hawes C: **Photoactivation of GFP reveals protein dynamics within the endoplasmic reticulum membrane.** *Journal of Experimental Botany* 2005, **57**:43-50.
6. Kwok EY, Hanson MR: **GFP-labelled Rubisco and aspartate aminotransferase are present in plastid stromules and traffic between plastids.** *Journal of Experimental Botany* 2004, **55**:595-604.
7. Kwok EY, Hanson MR: **In vivo analysis of interactions between GFP-labelled microfilaments and plastid stromules.** *BMC Plant Biology* 2004, **4**:1-9.
8. Flückiger R, Caroli de M, Piro G, Dalessandro G, Neuhaus J-M, Di Sansebastiano G-P: **Vacuolar system distribution in *Arabidopsis* tissues, visualized using GFP fusion proteins.** *Journal of Experimental Botany* 2003, **54**:1577-1584.
9. Brandizzi F, Fricker M, Hawes C: **A greener world: the revolution in plant bioimaging.** *Nature Reviews – Molecular Cell Biology* 2002, **3**:520-530.
10. Hanson MR, Köhler RH: **GFP imaging: methodology and application to investigate cellular compartmentation in plants.** *Journal of Experimental Botany* 2001, **52**:529-539.
11. Logan DC, Leaver CJ: **Mitochondria-targeted GFP highlights the heterogeneity of mitochondrial shape, size and movement within living plant cells.** *Journal of Experimental Botany* 2000, **51**:865-871.
12. Neuhaus J-M: **GFP as a marker for vacuoles in plants.** In *Annual Plant Reviews Vacuolar compartments Volume 5*. Edited by: Robinson DG. Sheffield Academic Press; 2000:254-269.
13. Tee CS, Marziah M, Tan CS, Abdullah MP: **Evaluation of different promoters driving the GFP reporter gene and selected target tissues for particle bombardment of *Dendrobium sonia*.** *Plant Cell Reports* 2003, **21**:452-458.
14. Fricker M, Runions J, Moore I: **Quantitative fluorescence microscopy: From art to science.** *Annual Reviews of Plant Biology* 2006, **57**:79-107.
15. Chiesa A, Rapizzi E, Tosello V, Pinton P, Virgilio de M, Fogarty KE, Rizzuto R: **Recombinant aequorin and green fluorescent protein as valuable tools in the study of cell signalling.** *Biochemical Journal* 2001, **355**:1-12.
16. Xu Y, Piston DW, Johnson CH: **A bioluminescence resonance energy transfer (BRET) system: Application to interacting circadian clock proteins.** *Proceedings of the National Academy of Sciences USA* 1999, **96**:151-156.
17. Fasano JM, Swanson SJ, Blancaflor EB, Dowd PE, Kao T, Gilroy S: **Changes in root cap pH are required for the gravity response of the *Arabidopsis* root.** *Plant Cell* 2001, **13**:907-921.
18. Miyawaki A, Llopis J, Heim R, McCaffery JM, Adams JA, Ikura M, Tsien RY: **Fluorescent indicators for calcium based on green fluorescent protein and calmodulin.** *Nature* 1997, **388**:882-887.
19. Miyawaki A, Griesbeck O, Heim R, Tsien RY: **Dynamic and quantitative Ca²⁺ measurements using improved cameleons.** *Proceedings of the National Academy of Science USA* 1999, **96**:2135-2140.
20. Allen GJ, Kwak JM, Chu SP, Llopis J, Tsien RY, Harper JF, Schroeder JI: **Cameleon calcium indicator reports cytoplasmic calcium dynamics in *Arabidopsis* guard cells.** *Plant Journal* 1999, **19**:735-747.
21. Gao D, Trewavas AJT, Knight MR, Sattelmacher B, Plieth C: **Self-reporting *Arabidopsis thaliana* expressing pH- and [Ca ²⁺]-indicators unveil ion dynamics in the cytoplasm and in the apoplast under abiotic stress.** *Plant Physiology* 2004, **134**:898-908.
22. Kuner T, Augustine GJ: **A genetically encoded ratiometric indicator for chloride: Capturing chloride transients in culture hippocampal neurons.** *Neuron* 2000, **27**:447-459.
23. Lorenzen I, Aberle T, Plieth C: **Salt stress – induced chloride flux: a study using transgenic *Arabidopsis* expressing a fluorescent anion probe.** *Plant Journal* 2004, **38**:539-544.
24. Kiegle E, Moore CA, Haseloff J, Tester J, Knight MR: **Cell-type-specific calcium responses to drought salt and cold in *Arabidopsis* roots.** *Plant Journal* 2000, **23**:267-278.
25. Miesenböck G, de Angelis DA, Rothman JE: **Visualizing secretion and synaptic transmission with pH-sensitive green fluorescent protein.** *Nature* 1998, **394**:192-195.
26. Plieth C, Sattelmacher B, Trewavas AJ, Hansen UP, Knight MR: **Engineering plants expressing calcium and pH indicators in the cytoplasm and the apoplast.** In *Plant Nutrition – Food security and sustainability of agro-ecosystems through basic and applied research (Proceedings of XIV International Plant Nutrition Colloquium, Hannover, Germany, 2001) – Developments in Plant and Soil Sciences – Series Volume 92.* Edited by: Horst. Kluwer Academic Publishers Dordrecht Netherlands; 2001:252-253.
27. Moseyko N, Feldman LJ: **Expression of pH-sensitive green fluorescent protein in *Arabidopsis thaliana*.** *Plant, Cell and Environment* 2001, **24**:557-563.
28. Shkrob MA, Yanushevich YG, Chudakov DM, Gurskaya NG, Labas YA, Poponov SY, Mudrik NN, Lukyanov S, Lukyanov KA: **Far-red fluorescent proteins evolved from a blue chromoprotein from *Actinia equina*.** *Biochemical Journal* 2005, **392**:649-654.
29. Shagin DA, Barsova EV, Yanushevich YG, Fradkov AF, Lukyanov KA, Labas YA, Semenova TN, Ugalde JA, Meyers A, Nunez JM, Widder EA, Lukyanov SA, Matz MV: **GFP-like proteins as ubiquitous metazoan superfamily: Evolution of functional features and structural complexes.** *Molecular Biology and Evolution* 2004, **21**:841-850.
30. Shaner NC, Campbell RE, Steinbach PA, Giepmans BNG, Palmer AE, Tsien RY: **Improved monomeric red, orange and yellow fluorescent proteins derived from *Discosoma sp*.** *Nature Biotechnology* 2004, **22**:1567-1572.
31. Wenck A, Pugieux C, Turner M, Dunn M, Stacy C, Tiozzo A, Dunder E, van Grinsven E, Khan R, Sigareva M, Wang WC, Reed J, Drayton P, Oliver D, Trafford H, Legris G, Rushton H, Tayab S, Launis K, Chang Y-F, Chen D-F-, Melchers L: **Reef-coral proteins as visual, nondestructive reporters for plant transformation.** *Plant Cell Reports* 2003, **22**:244-251.
32. Mazel CH, Lesser MP, Gorbunov MY, Barry TM, Farrell JH, Wyman KD, KFalkowski PG: **Green fluorescent proteins in caribbean corals.** *Limnology and Oceanography* 2003, **48**:402-411.
33. Papina M, Sakihama Y, Bena C, Woesik van R, Yamasaki H: **Seaparation of highly fluorescent proteins by SDS-PAGE in *Acropodiae* corals.** *Comparative Biochemistry and Physiology Part B* 2002, **131**:767-774.
34. Peelle B, Gururaja TL: **Characterization and Use of Green Fluorescent Proteins from *Renilla mulleri* and *Ptilosarcus guernyi* for the Human Cell Display of Functional Peptides.** *Journal of Protein Chemistry* 2001, **20**:507-519.
35. Bryan BJ, Szent-Gyorgyi C: **Luciferases, fluorescent proteins, nucleic acids encoding the luciferasses and fluorescent proteins and the use thereof in diagnostics, high throughput screening and novelty items.** *WIPO Patent, C12N 9/00* 1999.
36. Popov EG, Gavrilov IY, Pozin EYA, Gabbasov ZA: **Multiwavelength method for measuring concentration of free cytosolic calcium using the fluorescent probe indo-1.** *Archives of Biochemistry and Biophysics* 1988, **261**:91-96.
37. Tsien RY, Poenie M: **Fluorescence ratio imaging: a new window into intracellular ionic signaling.** *TIBS* 1986, **11**:450-455.
38. Bright GR, Fisher GW, Rogowska J, Taylor DL: **Fluorescence ratio imaging microscopy.** *Methods in Cell Biology* 1989, **30**:157-192.
39. Kneen M, Farinas J, Li Y, Verkman AS: **Green fluorescent protein as a non invasive intracellular pH indicator.** *Biophysical Journal* 1998, **74**:1591-1599.
40. Hanson GT, McAnaney TB, Park ES, Rendell MEP, Yarbrough DY, Chu S, Boxer SG, Montrose MH, Remington SJ: **Green fluorescent protein variants as ratiometric dual emission pH sensors. 1. Structural characterization and preliminary application.** *Biochemistry* 2002, **41**:15477-15488.
41. Felle HH: **The apoplast pH of the *Zea mays* root cortex as measured with pH-sensitive microelectrodes: aspects of regulation.** *Journal of Experimental Botany* 1998, **49**:987-995.

42. Grignon C, Sentenac H: **pH and ionic conditions in the apoplast.** *Annual Review of Plant Physiology and Plant Molecular Biology* 1991, **42:**103-128.

43. Griesbeck O, Baird GS, Campbell RE, Zacharias DA, Tsien RY: **Reducing the environmental sensitivity of yellow fluorescent protein.** *The Journal of Biological Chemistry* 2001, **276:**29188-29194.

44. Fricker MD, Parsons A, Tlalka M, Blancaflor E, Gilroy S, Meyer A, Plieth C: **Fluorescent probes for living plant cells.** In *Plant Cell Biology: A Practical Approach* 2nd edition. Edited by: Hawes C, Satiai-Jeunemaitre B. Oxford University Press Oxford; 2001:35-84.

45. Plieth C, Sattelmacher B, Hansen U-P: **Cytoplasmic Ca^{2+}-H$^+$-exchange buffers in green algae.** *Protoplasma* 1997, **198:**107-124. and Vol. 199: 223 (correction).

46. Felle HH: **pH regulation in anoxic plants.** *Annals of Botany* 2005, **96:**519-532.

47. Felle HH: **pH: Signal and messenger in plant cells.** *Plant Biology* 2001, **3:**577-591.

48. Felle HH: **Control of cytoplasmic pH under anoxic conditions and its implication for plasma membrane proton transport in Medicago sativa root hairs.** *Journal of Experimental Botany* 1996, **47:**967-973.

49. Ratcliffe RG: ***In vivo* NMR studies of the metabolic response of plant tissues to anoxia.** *Annals of Botany* 1997, **79(Supplement A):**39-48.

50. Gout E, Boisson A-M, Aubert S, Douce R, Bligny R: **Origin of the cytoplasmic pH changes during anaerobic stress in higher plant cells. Carbon-13 and phosphorous-31 nuclear magnetic resonance studies.** *Plant Physiology* 2001, **125:**912-925.

51. Flowers TJ: **Improving crop salt tolerance.** *Journal of Experimental Botany* 2004, **55:**307-319.

52. Apse MP, Blumwald E: **Engineering salt tolerance in plants.** *Current Opinion in Biotechnology* 2002, **13:**146-150.

53. Zhang H-X, Hodson JN, Williams JP, Blumwald E: **Engineering salt-tolerant *Brassica* plants: Characterization of yield and seed oil quality in transgenic plants with increased vacuolar sodium accumulation.** *Proceedings of the National Academy of Science USA* 2001, **98:**12832-12836.

54. Zhang H-X, Blumwald E: **Transgenic salt-tolerant tomato plants accumulate salt in foliage but not in fruit.** *Nature Biotechnology* 2001, **19:**765-768.

55. Spickett CM, Smirnoff N, Ratcliffe RG: **An *in vivo* nuclear magnetic resonance investigation of ion transport in maize (*Zea mays*) and *Spartina anglica* roots during exposure to high salt concentrations.** *Plant Physiology* 1993, **102:**629-638.

56. Felle HH: **The H$^+$/Cl$^-$ symporter in root hair cells of *Sinapis alba*.** *Plant Physiology* 1994, **106:**1131-1136.

57. Nakamura Y, Ogawa T, Kasamo K, Sakata M, Ohta E: **Changes in cytoplasmic and vacuolar pH in intact cells of mung bean root-tips under high-NaCl stress at different external concentrations of Ca^{2+} ions.** *Plant and Cell Physiology* 1992, **33:**849-85.

58. Katsuhara M, Kuchitsu K, Takeshige K, Tazawa M: **Salt stress-induced cytoplasmic acidification and vacuolar alkalization in *Nitellopsis obtusa* cells.** *Plant Physiology* 1989, **90:**1102-1107.

59. Fan TWM, Higashi RM, Norly J, Epstein E: ***In vivo* ^{23}Na and ^{31}P NMR measurement of a tonoplast Na$^+$/H$^+$ exchange process and its characteristics in two barley cultivars.** *Proceedings of the National Academy of Sciences USA* 1989, **86:**9856-9860.

60. Be-Hayyim G, Navon G: **Phosphorous-31 NMR studies of the wild-type and NaCl-tolerant *Citrus* cultured cells.** *Journal of Experimental Botany* 1985, **36:**1877-1888.

61. Sambrook J, Fritsch EF, Maniatis T: **Molecular cloning – a laboratoy manual.** *Volume 1–3*. Cold Spring Harbor Laboratory Press; 1989.

62. Ausubel FM, Brent R, Kingston RE, Moore DD, Seidman JG, Smith JA, Struhl K: **Short protocols in molecular biology.** Wiley New York; 1999.

63. Gleave AP: **A versatile binary vector system with a T-DNA organisational structure conducive to efficient integration of cloned DNA into the plant genome.** *Plant Molecular Biology* 1992, **20:**1203-1207.

64. Clough SJ, Bent AF: **Floral dip: a simplified method for Agrobacterium-mediated transformation of *Arabidopsis thaliana*.** *Plant Journal* 1998, **16:**735-743.

65. Plieth C, Trewavas AJ: **Reorientation of seedlings in the earth's gravitational field induces cytosolic calcium transients.** *Plant Physiology* 2002, **129:**786-796.

66. Grynkiewicz G, Poenie M, Tsien RY: **A new generation of Ca^{2+} indicators with greatly improved fluorescence properties.** *Journal of Biological Chemistry* 1985, **260:**3440-3450.